

ANDROMEDA IX: A NEW DWARF SPHEROIDAL SATELLITE OF M31

DANIEL B. ZUCKER,^{1,2} ALEXEI Y. KNIAZEV,¹ ERIC F. BELL,¹ DAVID MARTÍNEZ-DELGADO,¹ EVA K. GREBEL,^{1,3}
 HANS-WALTER RIX,¹ CONSTANCE M. ROCKOSI,⁴ JON A. HOLTZMAN,⁵ RENE A. M. WALTERBOS,⁵ JAMES ANNIS,⁶
 DONALD G. YORK,⁷ ŽELJKO IVEZIĆ,⁸ J. BRINKMANN,⁹ HOWARD BREWINGTON,⁹ MICHAEL HARVANEK,⁹ GREG HENNESSY,¹⁰
 S. J. KLEINMAN,⁹ JUREK KRZESINSKI,⁹ DAN LONG,⁹ PETER R. NEWMAN,⁹ ATSUKO NITTA,⁹ AND STEPHANIE A. SNEDDEN⁹

Received 2004 April 13; accepted 2004 July 23; published 2004 August 10

ABSTRACT

We report the discovery of a new dwarf spheroidal satellite of M31, Andromeda IX, based on resolved stellar photometry from the Sloan Digital Sky Survey (SDSS). Using both SDSS and public archival data, we have estimated its distance and other physical properties, and compared these to the properties of a previously known dwarf spheroidal companion, Andromeda V, also observed by SDSS. Andromeda IX is the lowest surface brightness galaxy found to date ($\mu_{V,0} \sim 26.8$ mag arcsec⁻²), and at the distance we estimate from the position of the tip of Andromeda IX's red giant branch, $(m - M)_0 \sim 24.5$ (805 kpc), Andromeda IX would also be the faintest galaxy known ($M_V \sim -8.3$).

Subject headings: galaxies: dwarf — galaxies: evolution —
 galaxies: individual (Andromeda V, Andromeda IX) — Local Group

1. INTRODUCTION

Hierarchical cold dark matter (CDM) models, while successful at large scales, predict too many low-mass dark subhalos to be consistent with the observed abundance of dwarf galaxies, by at least 1–2 orders of magnitude (e.g., Klypin et al. 1999; Moore et al. 1999; Benson et al. 2002a). This problem can be at least qualitatively addressed if star formation in low-mass subsystems were inhibited, for example, by photoionization in the early universe; this could lead to galaxy luminosity functions with shallow faint-end slopes at the present day (e.g., Somerville 2002; Benson et al. 2002b), with observed satellites embedded in much larger, more massive dark subhalos (Stoeckl et al. 2002).

Observational efforts to constrain the form of the luminosity function for faint galaxies are hindered by the extremely low surface brightnesses expected of such galaxies ($\mu_V \geq 26$ mag arcsec⁻²; e.g., Caldwell 1999; Benson et al. 2002a). Conducting a comprehensive ground-based survey for such diffuse objects would be extremely difficult even in nearby galaxy groups. Fortunately, in the case of the Local Group (LG), galaxies can be resolved into stars, allowing one to reach much fainter limits (e.g., Ferguson et al. 2002) and potentially place strong constraints on both the LG luminosity function and galactic formation models.

In this Letter, we report the discovery, using resolved stellar

data from the Sloan Digital Sky Survey (SDSS), of a new dwarf spheroidal companion to M31, one which is the lowest luminosity, lowest surface brightness galaxy found to date. For this work, we have assumed a distance to M31 of 760 kpc [$(m - M)_0 = 24.4$; van den Bergh 1999].

2. OBSERVATIONS AND DATA ANALYSIS

SDSS (York et al. 2000) is an imaging and spectroscopic survey that will eventually cover $\sim \frac{1}{4}$ of the sky. Drift-scan imaging in the five SDSS bandpasses (u, g, r, i, z ; Fukugita et al. 1996; Gunn et al. 1998; Hogg et al. 2001) is processed through data reduction pipelines to measure photometric and astrometric properties (Lupton et al. 2002; Stoughton et al. 2002; Smith et al. 2002; Pier et al. 2003) and to identify targets for spectroscopic follow-up. For this work, we used an SDSS scan along the major axis of M31, carried out on 2002 October 5 (see Zucker et al. 2004) and processed with the same pipeline as the First Data Release (Abazajian et al. 2003). In the following, all references to dereddening and conversion from the SDSS magnitudes to V, I magnitudes (for literature comparison) make use of Schlegel et al. (1998) and Smith et al. (2002), respectively.

This scan also included Andromeda V (And V; Armandroff et al. 1998), a known dwarf spheroidal (dSph) companion to M31; applying a simple photometric filter to the SDSS data, namely, selecting all stars with $i > 20.5$, reveals the presence of And V (Fig. 1a), even though it is barely visible in the summed SDSS g, r, i images of the field (Fig. 1c). This same filter yields another overdensity of faint stars (Fig. 1b) much closer to M31 on the sky, although it is not apparent in the summed SDSS image (Fig. 1d). In order to place some constraints on the nature of this stellar overdensity, we compared the color-magnitude diagrams (CMDs) of stars in the fields of And V and the new feature. For each object, we chose a circular region of radius $r = 2'$ and annuli with $8' \leq r \leq 10'$ as control fields for estimating foreground and field star contamination. Figure 2 shows the resulting Hess diagrams of And V and the stellar feature (*top panels*), the control fields, scaled by the area ratio of target and control fields (*middle panels*), and the difference of the two (*bottom panels*). The fact that the red giant

¹ Max-Planck-Institut für Astronomie, Königstuhl 17, D-69117 Heidelberg, Germany; zucker@mpia.de.

² Guest Investigator of the UK Astronomy Data Centre.

³ Astronomisches Institut, Universität Basel, Venusstrasse 7, CH-4102 Binningen, Switzerland.

⁴ Department of Astronomy, University of Washington, Box 351580, Seattle, WA 98195-1580.

⁵ Department of Astronomy, New Mexico State University, 1320 Frenger Mall, Las Cruces, NM 88003-8001.

⁶ Fermi National Accelerator Laboratory, P.O. Box 500, Batavia, IL 60510.

⁷ Department of Astronomy and Astrophysics, University of Chicago, 5640 South Ellis Avenue, Chicago, IL 60637.

⁸ Princeton University Observatory, Peyton Hall, Ivy Lane, Princeton, NJ 08544-1001.

⁹ Apache Point Observatory, P.O. Box 59, Sunspot, NM 88349.

¹⁰ US Naval Observatory, 3450 Massachusetts Avenue, NW, Washington, DC 20392-5420.

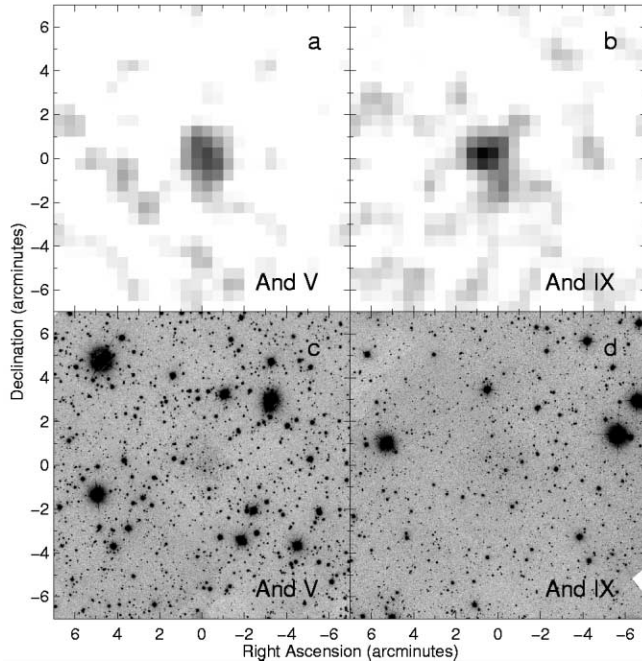


FIG. 1.—And V and And IX as seen by SDSS. (a, b) Spatial distribution of all SDSS stars with $i > 20.5$ in the fields of And V and And IX. The data in both panels were binned $30'' \times 30''$ and smoothed with a Gaussian (FWHM = $1''$). (c, d) Combined g , r , and i SDSS images of And V and And IX. Each panel spans $14' \times 14'$ and is oriented with north up and east to the left.

branch (RGB) in the new object extends to fainter magnitudes than that of And V is explained by the significant differences in seeing ($\sim 1''.3$ vs. $\sim 1''.9$ in the i band) and the consequent differences in completeness near the faint detection limit. RGB fiducials for Galactic globular clusters spanning a wide range of metallicities are overplotted. The similarity between the two bottom panels is striking, as both And V and the new stellar structure show rather narrow, blue RGBs. While individual photometric errors and uncertainties in the transformations between g, r, i and V, I photometric systems do not allow us to assign a specific metallicity to either object, the blue color is significant; And V has a metallicity of $[\text{Fe}/\text{H}] \lesssim -2$ (Davidge et al. 2002; Guhathakurta et al. 2000), and the RGB color of the new feature suggests a comparably low metallicity.

3. A NEW COMPANION OF M31

The stars in this new overdensity exhibit magnitudes and colors consistent with their being near the tip of the RGB (TRGB), at approximately the distance of M31 and its satellites. Their CMD is distinct from the surrounding field (see Fig. 2) and is in fact rather similar to that of And V, the known dSph satellite of M31 referred to above; the similar angular size and extremely low surface brightness are further indications that this structure is also a dSph galaxy. Following the nomenclature of van den Bergh (1972), and in light of the recently proposed Andromeda VIII (Morrison et al. 2003), we have named the new object Andromeda IX (And IX).

We applied the methodology of Kniazev et al. (2004) to the SDSS data; briefly, this entailed masking foreground stars and background galaxies and subtracting a fitted sky level prior to measuring integrated fluxes and central surface brightnesses. The properties of And V derived in this way are shown in the first column of Table 1; Caldwell (1999) found a central surface brightness $\mu_{0,V} = 24.8 \pm 0.2$ and an integrated magnitude

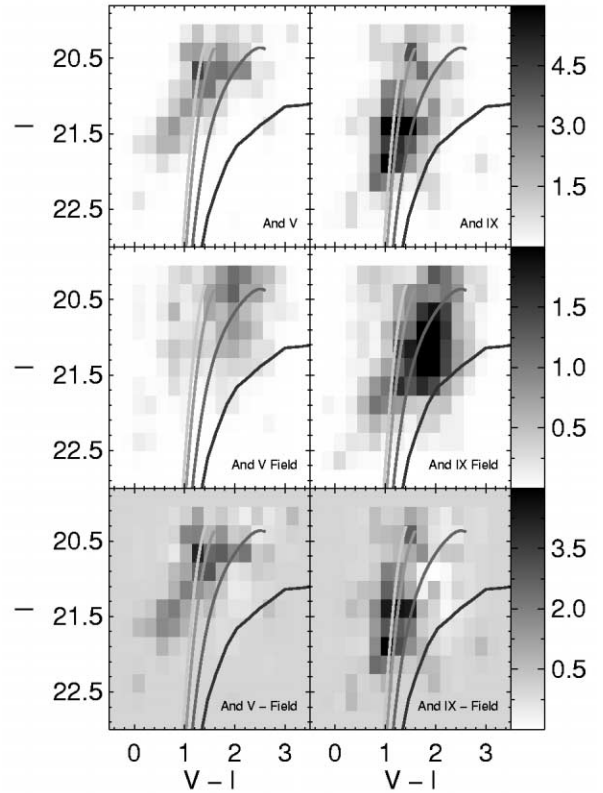


FIG. 2.—Hess diagrams of And V (left) and And IX (right) from SDSS data. *Top panels*: Stars within a $2'$ radius of the center of each galaxy. *Middle panels*: Control field for each galaxy (an annulus spanning $8' - 10'$ from each galaxy center). *Bottom panels*: Hess diagrams for each galaxy, minus the control-field Hess diagram (scaled by the ratio of areas). Data are dereddened, converted to V, I , binned by 0.25 in I and $V - I$, and smoothed with a Gaussian filter. The number of stars in each bin is indicated by the gray scale to the right of each pair of panels. Fiducial sequences are overplotted for Galactic globular clusters with metallicities of (left to right) $[\text{Fe}/\text{H}] = -2.2$ (M15), -1.6 (M2), -0.7 (47 Tuc), and -0.3 (NGC 6553; Da Costa & Armandroff 1990; Sagar et al. 1999), shifted to the adopted M31 distance modulus of 24.4 ; for NGC 6553, a distance modulus of 13.7 and a reddening of $E(V - I) = 0.95$ were assumed (Sagar et al. 1999).

$V_{\text{tot}} = 15.42 \pm 0.14$ for And V, both in good agreement with our results. However, owing to And IX's extremely low surface brightness, no unresolved luminous component was detected in the SDSS data. Consequently, we used the data for And V (in which unresolved luminosity could be quantified) to estimate corrections for And IX surface brightness measurements based on resolved stars alone: 3.1 ± 0.2 , 2.6 ± 0.2 , and 2.3 ± 0.2 mag for the g , r , and i bands, respectively. These

TABLE 1
PROPERTIES OF AND V AND AND IX

Parameter ^a	And V	And IX _{SDSS}	And IX _{INT}
R.A. (J2000.0)	01 10 16.2	00 52 53.0	00 52 52.8
Decl. (J2000.0)	+47 37 52	+43 11 45	+43 12 00
A_V (mag)	0.41	0.26	0.26
$\mu_{0,V}$ (mag)	25.02 ± 0.11	26.3 ± 0.5	26.77 ± 0.09
V_{tot} (mag)	15.32 ± 0.06	...	16.17 ± 0.06
$(m - M)_0$ (mag)	24.53 ± 0.20	...	24.48 ± 0.20
$M_{\text{tot},V}$ (mag)	-9.2	...	-8.3

^a Units of right ascension are hours, minutes, and seconds, and units of declination are degrees, arcminutes, and arcseconds. Surface brightnesses and integrated magnitudes are corrected for the mean galactic foreground reddenings, A_V , shown.

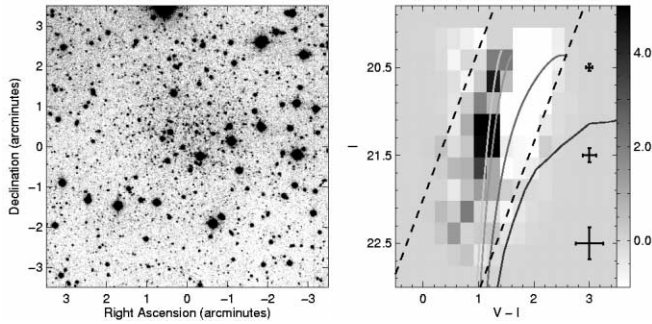


FIG. 3.—And IX as seen by the INT. *Left*: 800 s archival V-band image, covering $7' \times 7'$. *Right*: Dereddened, control-field-subtracted Hess diagram of And IX. The dashed lines indicate the limits of the color-magnitude region selected from both SDSS and INT data for analysis of the I -band luminosity function (see Fig. 4); the crosses show typical photometric errors for stars over a range of I -band magnitudes. Binning, smoothing, and the overplotted fiducials are the same as for Fig. 2. The gray scale indicates the number of stars in each bin.

values are consistent with those derived in Zucker et al. (2004) from observations of the Pegasus dwarf irregular and the Draco dSph. Applying these corrections to the resolved-star surface brightness profile calculated for And IX, we obtained dereddened central surface brightnesses of 27.0 ± 0.5 , 26.1 ± 0.5 , and 25.8 ± 0.3 mag arcsec $^{-2}$ in g , r , and i (26.3 ± 0.5 in V , second column of Table 1). Unfortunately, the small number of stars detected in And IX (an excess of ~ 60 stars above the mean field density in a $2'$ -radius region) made it impossible to reliably measure an integrated magnitude for And IX from the SDSS data.

In order to learn more about And IX, we analyzed two images covering the region of the galaxy from the Isaac Newton Group (ING) Archive. These images, 800 s exposures in V and i' filters, were taken with the 2.5 m Isaac Newton Telescope (INT) on La Palma. The INT images are significantly deeper than those from SDSS; in fact, And IX is readily visible in the INT V -band image (Fig. 3, *left panel*). We reduced the data using standard IRAF tasks, obtained stellar photometry with DAOPHOT (Stetson 1994), used our SDSS data to bootstrap-calibrate this photometry to V and I magnitudes, and dereddened the photometric data.

We then generated Hess diagrams for stars from the same $2'$ -radius region around the center of And IX as for the SDSS data and from a nearby $11' \times 11'$ control field, scaling the control-field diagram by the area ratio of target and control fields. The right panel of Figure 3 shows the difference of these two Hess diagrams. As in Figure 2, the control-field-subtracted Hess diagram for And IX generated from the INT data reveals a narrow, blue RGB, confirming that the observed stellar population of And IX is distinct from that of the projected field and quite metal-poor ($[\text{Fe}/\text{H}] \lesssim -2$).

The deeper INT images also provided better stellar number statistics and allowed us to directly measure the unresolved luminosity of And IX. Applying the same techniques as for the SDSS data, we determined the physical parameters listed in the third column of Table 1. As a check on this method, we also tried subtracting the point-spread functions of, rather than masking, foreground stars from the archival images before measuring physical parameters, but the results differed by $\lesssim 0.05$ mag from our initial estimates (i.e., within the quoted measurement errors). Of particular note are the dereddened values for the central surface brightness, $\mu_{0,V} = 26.77 \pm 0.09$, and the integrated magnitude, $V_{\text{tot}} = 16.17 \pm 0.06$; not only do they confirm And IX

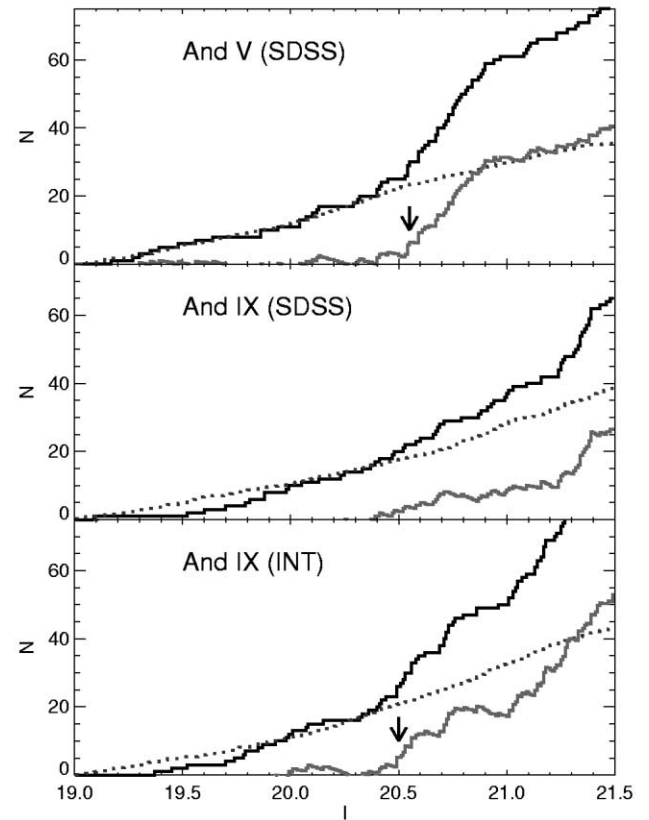


FIG. 4.— I -band luminosity functions for And V and And IX. *Top*: Cumulative I -band luminosity function for SDSS stars within a $2'$ radius of the center of And V (black solid line), the scaled cumulative I -band luminosity function for the corresponding control field (black dotted line), and the difference of the two (gray solid line). The arrow indicates the presumed location of the TRGB, $I = 20.55$. *Middle*: Same as in the top panel, but for SDSS stars within a $2'$ radius of the center of And IX. *Bottom*: Same as in the top panel, but for INT stars within a $2'$ radius of the center of And IX. The arrow indicates the presumed location of the TRGB, $I = 20.50$. All luminosity functions—for both target and control fields—are for dereddened stars falling in the color-magnitude region illustrated in the right panel of Fig. 3.

as the lowest surface brightness galaxy found to date, but, at the distance of M31, And IX would also be the lowest luminosity galaxy known.

The true distance to And IX is thus of considerable importance. One method of measuring the distance to resolved, metal-poor galaxies like And IX is by determining the magnitude of the TRGB (e.g., Lee et al. 1993). We generated cumulative dereddened I -band luminosity functions for stars within the central $2'$ radius of And V and And IX, selecting only stars from the color-magnitude region shown by the dashed lines in the right panel of Figure 3. We did the same for the respective control fields, scaling by the ratio of target and control-field areas, and then subtracted the appropriate control-field luminosity function from that of each galaxy (Fig. 4). The field-star-subtracted luminosity function begins to rise significantly at $I \sim 20.55 \pm 0.15$ in And V and $I \sim 20.50 \pm 0.15$ in And IX, which we interpret as the TRGB in each galaxy. Assuming metallicities of $[\text{Fe}/\text{H}] = -2.2$ and TRGB colors of $(V - I)_{\text{TRGB}} = 1.2$ for both galaxies, we applied the empirical formulae of Da Costa & Armandroff (1990) to derive a calibration for the TRGB distance: $(m - M)_0 = I_{\text{TRGB}} + 3.98$. Thus, we calculate And IX's distance modulus to be ~ 24.48 (790 kpc), with errors on the order of 0.2 mag ($\sim \pm 70$ kpc). While this is a somewhat crude estimate, it is worth noting that our dis-

tance to And V, $(m - M)_0 \sim 24.53$ (805 kpc), is in excellent agreement with that obtained by Armandroff et al. (1998), 24.55 (810 kpc). The angular separation of And IX from the center of M31 is $\sim 2''.6$, which at an M31 distance of 760 kpc translates to a projected separation of 34 kpc; assuming that And IX is some 30 kpc more distant than M31 places And IX 45 kpc from the center of M31. Thus, barring an improbably high relative velocity, And IX is a bound satellite of M31. At a distance modulus of 24.48, the dereddened integrated magnitude $V_{\text{tot}} = 16.17$ translates to an absolute magnitude of $M_V \sim -8.3$, making And IX 0.6 mag (a factor of 1.7) fainter than the least luminous galaxy known, the Ursa Minor dSph (Kleyna et al. 1998).

4. DISCUSSION

And IX is the lowest surface brightness, lowest luminosity galaxy found to date, with a metallicity comparable to the least chemically evolved stellar systems in the LG; its distance from the center of M31, ~ 45 kpc, places it well within, e.g., the virial radius (272 kpc) assumed by Benson et al. (2002a) in their models, indicating that it is in all likelihood a satellite of that galaxy. At an absolute magnitude of $M_V \sim -8.3$ ($\sim 2 \times 10^5 L_\odot$), And IX is comparable in luminosity to many globular clusters, although 2 orders of magnitude larger ($r \gtrsim 500$ pc).

Given that current hierarchical CDM models for galaxy formation still generate a satellite galaxy luminosity function that rises at low luminosities (albeit with a shallower slope than some earlier models), the discovery of And IX raises some interesting questions. Is And IX a rarity, one of a small number of such extremely low luminosity galaxies in the LG, with the vast majority of the predicted large numbers of low-mass subhalos surviving only as dark matter? Or could And IX be the tip of the iceberg, representative of a large population of low-luminosity dwarf satellites that have remained undetected because of their extremely low surface brightnesses (e.g., Benson et al. 2002a)?

The discovery of And IX (like that of And NE; Zucker et al. 2004) also highlights the capabilities of large-scale imaging surveys with uniform photometry, like SDSS, for detecting incredibly diffuse stellar structures in the LG using their resolved stellar components (see Willman et al. 2002 for a detailed discussion). If And IX is but one of a large population of extremely faint M31 satellites, it is quite likely that further analysis of the SDSS data will yield more such objects, bringing the observed galaxy luminosity function into better agreement with model predictions.

D. B. Z. acknowledges support from a National Science Foundation International Postdoctoral Fellowship. E. F. B. acknowledges the financial support provided through the European Community's Human Potential Program under contract HPRN-CT-2002-00316, SISCO. This research has made use of data from the ING archive.

Funding for the creation and distribution of the SDSS Archive has been provided by the Alfred P. Sloan Foundation, the Participating Institutions, the National Aeronautics and Space Administration, the National Science Foundation, the US Department of Energy, the Japanese Monbukagakusho, and the Max Planck Society.

The SDSS¹¹ is managed by the Astrophysical Research Consortium (ARC) for the Participating Institutions. The Participating Institutions are the University of Chicago, Fermilab, the Institute for Advanced Study, the Japan Participation Group, the Johns Hopkins University, Los Alamos National Laboratory, the Max-Planck-Institute for Astronomy (MPIA), the Max-Planck-Institute for Astrophysics (MPA), New Mexico State University, the University of Pittsburgh, Princeton University, the US Naval Observatory, and the University of Washington.

¹¹ The SDSS Web site is <http://www.sdss.org>.

REFERENCES

- Abazajian, K., et al. 2003, *AJ*, 126, 2081
 Armandroff, T. E., Davies, J. E., & Jacoby, G. H. 1998, *AJ*, 116, 2287
 Benson, A. J., Frenk, C. S., Lacey, C. G., Baugh, C. M., & Cole, S. 2002a, *MNRAS*, 333, 177
 Benson, A. J., Lacey, C. G., Baugh, C. M., Cole, S., & Frenk, C. S. 2002b, *MNRAS*, 333, 156
 Caldwell, N. 1999, *AJ*, 118, 1230
 Davidge, T. J., Da Costa, G. S., Jørgensen, I., & Allington-Smith, J. R. 2002, *AJ*, 124, 886
 Da Costa, G. S., & Armandroff, T. E. 1990, *AJ*, 100, 162
 Ferguson, A. M. N., Irwin, M. J., Ibata, R. A., Lewis, G. F., & Tanvir, N. R. 2002, *AJ*, 124, 1452
 Fukugita, M., Ichikawa, T., Gunn, J. E., Doi, M., Shimasaku, K., & Schneider, D. P. 1996, *AJ*, 111, 1748
 Guhathakurta, P., Reitzel, D. B., & Grebel, E. K. 2000, *Proc. SPIE*, 4005, 168
 Gunn, J. E., et al. 1998, *AJ*, 116, 3040
 Hogg, D. W., Finkbeiner, D. P., Schlegel, D. J., & Gunn, J. E. 2001, *AJ*, 122, 2129
 Kleyna, J. T., Geller, M. J., Kenyon, S. J., Kurtz, M. J., & Thorstensen, J. R. 1998, *AJ*, 115, 2359
 Klypin, A., Kravtsov, A. V., Valenzuela, O., & Prada, F. 1999, *ApJ*, 522, 82
 Kniazev, A. Y., Grebel, E. K., Pustilnik, S. A., Pramskij, A. G., Kniazeva, T. F., Prada, F., & Harbeck, D. 2004, *AJ*, 127, 704
 Lee, M. G., Freedman, W. L., & Madore, B. F. 1993, *ApJ*, 417, 553
 Lupton, R. H., Ivezić, Ž., Gunn, J. E., Knapp, G., Strauss, M. A., & Yasuda, N. 2002, *Proc. SPIE*, 4836, 350
 Moore, B., Ghigna, S., Governato, F., Lake, G., Quinn, T., Stadel, J., & Tozzi, P. 1999, *ApJ*, 524, L19
 Morrison, H. L., Harding, P., Hurley-Keller, D., & Jacoby, G. 2003, *ApJ*, 596, L183
 Pier, J. R., Munn, J. A., Hindsley, R. B., Hennessy, G. S., Kent, S. M., Lupton, R. H., & Ivezić, Ž. 2003, *AJ*, 125, 1559
 Sagar, R., Subramaniam, A., Richtler, T., & Grebel, E. K. 1999, *A&AS*, 135, 391
 Schlegel, D. J., Finkbeiner, D. P., & Davis, M. 1998, *ApJ*, 500, 525
 Smith, J. A., et al. 2002, *AJ*, 123, 2121
 Somerville, R. S. 2002, *ApJ*, 572, L23
 Stetson, P. B. 1994, *PASP*, 106, 250
 Stoehr, F., White, S. D. M., Tormen, G., & Springel, V. 2002, *MNRAS*, 335, L84
 Stoughton, C., et al. 2002, *AJ*, 123, 485
 van den Bergh, S. 1972, *ApJ*, 171, L31
 ———. 1999, *A&A Rev.*, 9, 273
 Willman, B., Dalcanton, J., Ivezić, Ž., Jackson, T., Lupton, R., Brinkmann, J., Hennessy, G., & Hindsley, R. 2002, *AJ*, 123, 848
 York, D. G., et al. 2000, *AJ*, 120, 1579
 Zucker, D. B., et al. 2004, *ApJ*, 612, L117